Induced supershear microseismic event with rupture directivity and superimposed attenuation effects

Miłosz Wcisło, František Staněk, František Gallovič, Shaojiang Wu and Ivan Pšenčík

We investigate combined rupture directivity and attenuation effects on direct waveforms of an induced microseismic event recorded in China. The event with M_W~1 located at the depth of ~3800 m depth was recorded during the hydraulic fracturing of shale reservoir in North China, by a star-like surface array with 12 arms and a total of 1771 vertical component geophones, see Figure 1a. Rupture directivity is a fundamental effect that is well known for large natural earthquakes (Koketsu et al., 2016). Its observation in microseismic events is difficult due to usually insufficient station coverage and stronger effects of attenuation along wave propagation paths. Due to attenuation effects (described by global absorption factor t^*), amplitudes and frequency content of direct arrivals characterized by peak frequencies f_{peak}, that initially vary with direction, start to converge to similar values for the same offsets (Eisner et al., 2013).

From the dataset we selected 629 receivers (gray dots in Fig.1a) that provide clear symmetrical P-wave pulses with high signal-to-noise ratio that allowed reliable f_{peak} measurement. Measured f_{peak} shown in Figure 1b showed strong azimuthal pattern that was difficult to explain by variations of attenuation caused by differences in elevation of receivers with similar offsets. We suspected that the pattern could be caused by the rupture directivity. Using additional 98 amplitude picks (magenta dots in Fig. 1a), we computed ray-based Green's functions and performed full moment tensor inversion of P-wave arrival amplitudes. The analyzed event is of a strike-slip type with two nearly vertical nodal planes oriented in the NW-SE direction (strike: 326°, dip: 85°, rake: -180°) and in the NE-SW direction (strike: 236°, dip: 90°, rake: -5°), with the double couple (DC) component of 66%.

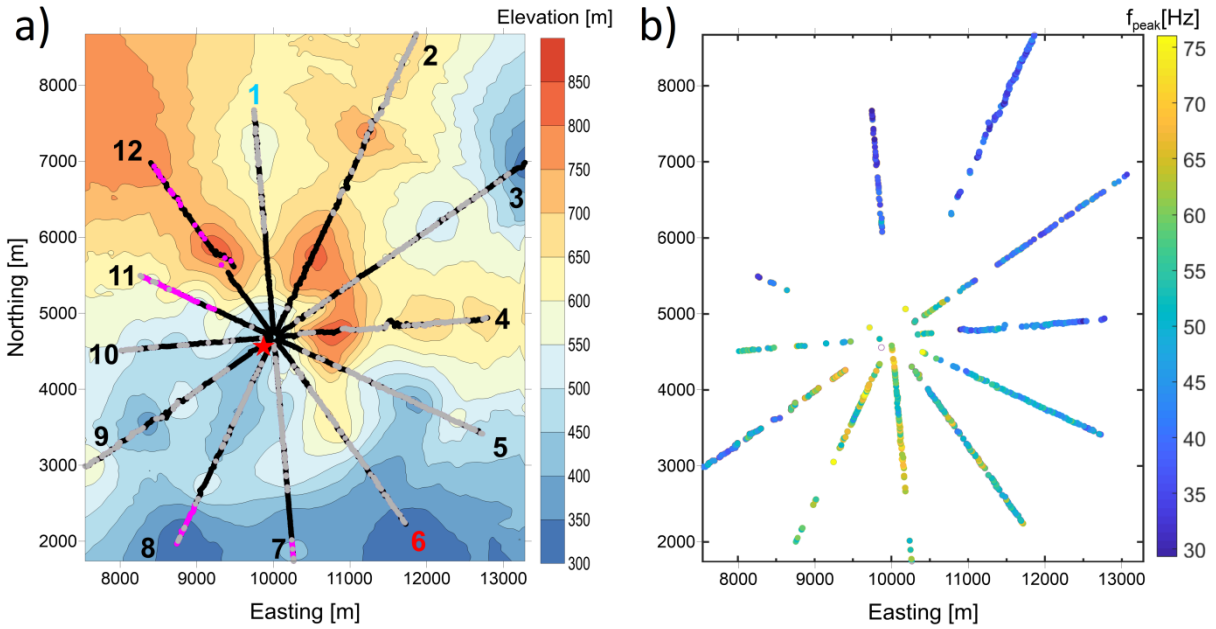

Figure 1. a) Map of the area of investigation including elevation. Dots show the positions of 1771 receivers that make up a star-like surface monitoring array with 12 arms. Receivers with clear, single P-wave arrival are in grey, receivers with additionally picked amplitude of P-wave arrival used in source mechanism inversion amplitudes are in magenta. The red star in the center represents the epicenter of the studied event. b) distribution of measured from direct arrivals peak frequencies.

We performed synthetic modelling of the peak frequencies for the investigated event at the receivers selected for peak frequency measurement locations. We grid searched for source rupture duration, rupture propagation direction, quality factor Q, and rupture velocity summarized in Table 1. The modelling provides better fit to measured f_{peak} from the data if rupture direction is included in the search than if the point source assumption (no directivity) is used. The best fit that explains broad range of measured f_{peak} is obtained if we allow the event to have supershear rupture propagation. Still, the highest values of the measured f_{peak}, which are found south to the event, are not fully explained by our modelling with single effective (average) Q in the whole area. The possible explanation of these high values is possible smaller thickness of the uppermost layer in the area – the elevation in this part of the array is lower. Near surface layer is usually the most attenuative. The modelling allowed us to choose the nodal plane of the event which is located in the NW-SE direction (strike: 326°, dip: 85°, rake: -180°).

		misfit	Q inverted	minimum / maximum synthetic f_{peak} value	range of observed f_{peak} explained (5^{th}-95^{th} percentile)
no directivity	constant peak frequencies	36,6	-	48 / 48	0%
	constant corner frequency (200hz)	18,1	150	37 / 53	49%
directivity	$V_{rupture}$/Vs=0.9	15,0	170	36 / 53	56%
	$V_{rupture}$/Vs=1.5	13,4	150	32 / 56	81%

Table 1. Summary of results of the modelling for 4 cases of different model complexity – from modelling that does not include attenuation and directivity effects, to the case, which includes attenuation and allows supershear rupture propagation. L2 misfit based on the differences of logarithms of measured and modelled f_{peak} is basis of misfit computation. Percentage of explained range of observed f_{peak} is computed using range from 5th to 95^{th} percentile of observed in the data f_{peak}.

Acknowledgements

We thank the project Research Project 20-06887S of the Grant Agency of the Czech Republic, the project SVV 260581 of the Charles University, and the research project CzechGeo/EPOS LM2015079 of the Ministry of Education, Youth and Sports of the Czech Republic for support.

References:

Eisner, L., Gei, D., Hallo, M., Opršal, I. Ali, M.Y., 2013. The peak frequency of direct waves for microseismic events, Geophysics. 78, A45-A49.

Koketsu, K., Miyake, H., Guo, Y. et al., 2016. Widespread ground motion distribution caused by rupture directivity during the 2015 Gorkha, Nepal earthquake. Scientific Reports, 6, 28536.